

Fragments from uranium irradiated by 2.1 GeV/nucleon deuterons and alpha particles*

A. M. Zebelman, A. M. Poskanzer, J. D. Bowman,[†] R. G. Sextro, and V. E. Viola, Jr.[‡]

Lawrence Berkeley Laboratory, University of California, Berkeley, California 94720

(Received 9 December 1974)

Energy spectra at 90° in the laboratory were obtained for He, Li, Be, and B fragments from a uranium target irradiated with 4.9 GeV protons and 2.1 GeV/nucleon deuterons and α particles. Data at 25 and 155° were also obtained with the proton and α particle beams. In comparing the incident deuteron data with the incident proton data, it was found that the cross sections were a factor of 1.5 higher but the shapes of the energy spectra were unchanged. However, with incident α particles it was found that the cross sections were a factor of 3 to 4 larger, and the energy spectra were somewhat broadened indicating that the effective Coulomb barriers are 15% lower, and the apparent temperatures 1.5 MeV higher. It is concluded that in the α particle irradiations the deposition energies are larger than with either incident protons or incident deuterons.

NUCLEAR REACTIONS U(p, x), $E=4.9$ GeV; U(α, x), $E=2.1$ GeV/nucleon; ^4He , ^6He , ^6Li , ^7Li , ^7Be , ^9Be , ^{10}Be measured E_x at 90°, $\sigma(\theta)$, σ ; ^8Li , ^9Li , ^{11}Be , ^{12}Be estimated σ . U(d, x), $E=2.1$ GeV/nucleon; ^4He , ^7Li , ^7Be , ^9Be , ^{10}Be measured E_x at 90°, estimated σ ; ^6He , ^6Li , ^8Li , ^9Li estimated σ .

I. INTRODUCTION

Recent studies have begun to explore the interaction of accelerator produced relativistic heavy ions with nuclei.¹ It appears so far that most of the products fall into two classes: those with high velocities in the laboratory, clearly fragments from the projectile, and those with low velocities in the laboratory, clearly fragments from the target. Several experiments on projectile fragmentation already have been carried out using techniques of high-energy physics.² A preliminary study of target fragmentation using plastic track detectors has been published.³ The present experiment is a ΔE - E counter telescope study of the products of target fragmentation.

The general features of the interaction of high-energy protons with nuclei are well known. They are usually understood in terms of an intranuclear cascade followed by an evaporation stage. An important aspect of these reactions which has emerged recently is that the gross features of this interaction are independent of proton bombarding energy from a few GeV up to 300 GeV.⁴ That is, it appears that above a few GeV, increasing the proton energy does not deposit any more energy in the target nucleus. The orientation of the present work is to determine if the gross features change when one keeps the energy of the projectile at a few GeV/nucleon but increases the mass of the projectile. The preliminary results of Sullivan *et al.*³ indicate that significant

changes occur.

Some data exist for target spallation induced by α particles with energies of 200 MeV/nucleon and lower.⁵ Except for an average factor of 2 increase in production cross sections, only small differences from the corresponding data from proton-induced reactions are observed. However, at 2 GeV/nucleon the situation may well be different because of the strong forward peaking of the nucleon-nucleon scattering cross sections.

We have previously made extensive studies of the energy spectra and angular distributions of He through Mg fragments from heavy targets irradiated by high-energy protons.^{6,7} This work shows that the energy spectra of the products Li and heavier are sensitive indicators of high deposition energies in the nucleus. Thus a comparison of the energy spectra of these fragments produced by heavy ions and protons should bear on this problem of energy deposition. Also, if some kind of collective interaction, such as a shock wave,⁸ becomes important for heavier projectiles the study of the properties of these particular fragments might be significant.

In the present work energy spectra and crude angular distributions were measured for He to B fragments from a uranium target irradiated by the 2.1 GeV/nucleon deuteron and α beams from the Bevatron. In order to allow a careful comparison with proton-induced reactions, data were remeasured with the same equipment using 4.9 GeV protons.

II. EXPERIMENTAL

A. General

Most of the experimental details are described more fully in Ref. 6. The external beam of the Bevatron passed through a scattering chamber 91 cm in diameter. The typical on-target beam profile was 1.3 cm wide by 1.6 cm high with average intensities of 4×10^{10} deuterons/pulse and 7×10^8 α /pulse at rates of 10 pulses per min. The target assembly located in the center of the scattering chamber consisted of a 10.4-mg/cm²-thick U target, 3.8 cm wide and 2.5 cm high, fastened at its edges to a 1-mg/cm²-thick Mylar sheet which in turn was attached to a frame 16.5 cm wide by 8.9 cm high. The angle of the normal of the target with respect to the beam was either 55° or 125°.

In general, the detector telescopes used consisted of a transmission ΔE detector, an E detector, and an anticoincidence detector. The detectors were phosphorous-diffused silicon except for a 1500- μ m-thick E detector which was lithium-drifted silicon.

Signals from the detector telescope were used in a particle identifier system of the power-law type. The particle identifier (PI) signals and total energy (E_T) signals were sent to a small computer which stored them on magnetic tape, event-by-event, for off-line analysis and in the computer memory as histograms. The energy spectra of selected PI peaks were monitored during the experiment. The counting rate versus time during the 1-sec beam burst of the accelerator was also displayed by the computer. A tagged pulser signal was sent through the electronics during data collection which allowed monitoring of system stability.

The beam intensity was monitored with an ionization chamber upstream from the scattering chamber. The ion chamber was calibrated by irradiating a polystyrene target in the scattering chamber using the well known $^{12}\text{C}(p, pn)^{11}\text{C}$ reaction. The stability of the ion chamber over the period of an experiment was 1%.

B. Specific experimental details

The experiment was carried out in two parts. In the first part a telescope with a 48- μ m-thick ΔE counter was used. The data from the deuteron-induced reactions appeared to be very similar to those from the proton-induced reactions but the α -induced data exhibited interesting differences at both high and low fragment energies. Thus a second set of data was taken using two

telescopes, one having a 22- μ m-thick ΔE detector and the other a 1.5-mm-thick E detector. By this time the introduction of a multiwire proportional chamber just downstream of our target allowed the Bevatron beam position to be maintained sufficiently stable so that the ion chamber could be used effectively to monitor the beam intensity. The data collected in the deuteron irradiation were not remeasured. Only the data from the second α bombardment are presented here since the early data agreed within the errors and also were not as complete.

1. Deuteron and associated proton bombardments

Copper collimators 0.4 mm thick and 8 mm in diameter were placed in front of the ΔE and E detectors, with the distance from the E collimator to the center of the target equal to 27 cm. Table I lists the thicknesses of the detectors in the telescope and gives the lower level discriminator settings on the E detectors which determined the low-energy electronic cutoff in the fragment spectra. Although the telescope was movable, time allowed good energy spectra to be collected only at 90° in the laboratory.

2. α and associated proton bombardments

Two fragment telescopes were employed simultaneously in the measurements. The thick telescope contained detectors chosen to measure the high-energy portions of the fragment spectra while the thin telescope contained detectors chosen to measure the low-energy portions. The thick telescope copper collimators were 1.0 mm thick and were 8 mm in diameter. The thin telescope copper collimators were 0.5 mm thick and were 4 mm wide by 6 mm high. The thicknesses of the detectors in these telescopes are also given in Table I along with the lower level discriminator settings for the E detectors.

The distances from the center of the target to the E collimators for the thick and the thin telescopes were equal to 27 cm both for the proton irradiations and for the angular distribution measurements with the α particle beam. The lower

TABLE I. Telescopes used in this study. The numbers given are the thicknesses in microns of the ΔE and E counters, followed in parentheses by the lower discriminator setting in MeV of the E counter.

Beams	Telescope	Detectors
$d; p$	Medium	48-382 (3)
$\alpha; p$	Thick	177-1500 (5)
	Thin	22-205 (2.1)

beam intensity obtained with the α beam required that the telescopes be moved in to 12 cm from the target for the measurement of the 90° energy spectra. Brief measurements at the larger distance showed that no spectrum distortion occurred with the larger solid angle. Data were collected at laboratory angles of 25° , 90° , and 155° for each telescope. Several shorter runs at the beginning, middle, and end of the experiment were done with both telescopes at 90° to check system stability.

C. Data processing

Following completion of the experiments the data were resorted with modified PI windows, if necessary, and data taken in different runs at the same laboratory angle were combined. The histograms were written onto a magnetic tape which was then processed on a CDC 7600 computer. The channel numbers were transformed to energies and the data were then corrected for the energy lost in half the apparent target thickness, and also for the dead layers in the detectors. The range-energy formalism of Bichsel and Tschaler⁹ was used to make these corrections in the same manner as described in Ref. 6.

Cross sections were obtained in the case of the proton bombardment by requiring that the differential cross section at 90° for the production of

^4He be 297 mb/sr as previously measured for 5.5 GeV protons. It is thought that there is very little change in this cross section from 4.9 to 5.5 GeV. The deuteron- and α -particle-induced data were normalized to the proton-induced data by making the reasonable assumption that the ion chamber calibration for the different beams varied as the theoretical dE/dx values of the particles. The ratio of the dE/dx values of protons to deuterons is 1.0 and for α particles to protons is 3.9. A polystyrene foil irradiation was also performed in the α beam. Using these assumptions one calculates¹⁰ that the $^{12}\text{C}(\alpha, \alpha n)^{11}\text{C}$ cross section decreases only about 10% from 0.92 to 8.4 GeV.

Linear graphs of the energy spectra were extrapolated to high and low energies for the small amount of unmeasured cross section and were integrated to give angular distributions. These cross sections were then plotted versus the cosine of their laboratory angles and the lines connecting them integrated to give total cross sections.

III. RESULTS

A comparison of the fragment energy spectra at 90° in terms of ratios of incident deuteron-to-proton and incident α -to-proton double differential cross sections is made in Fig. 1. The differences are striking. The behavior of the fragment spec-

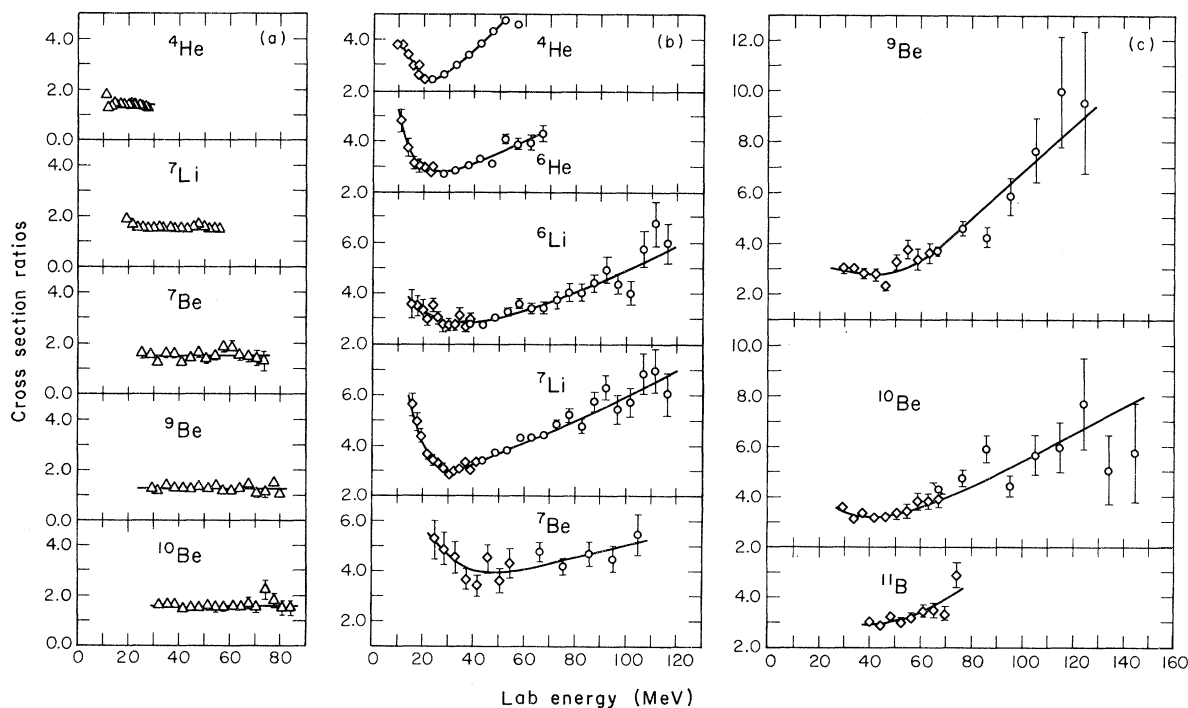


FIG. 1. Ratios of energy spectra at 90° in the laboratory for (a) incident deuterons to incident protons, and (b), (c) for incident α particles to incident protons.

tra from the deuteron beam is the same within experimental error as that from the proton beam. It should be noted in the figure that the cross sections of the deuteron-induced reactions are somewhat larger than those resulting from proton bombardment. On the other hand the α -induced reactions, also shown in Fig. 1, exhibit both markedly broadened fragment energy spectra and larger cross sections relative to the proton data.

The energy spectra from the α particle reactions and the proton reactions are shown in Fig. 2. The peak cross sections of the proton-induced reactions have been normalized to those of the α -induced reactions in order to illustrate the more prominent high-energy tails and somewhat increased yields at low energies in the α data. Because of the low counting rates a fairly thick target was necessary which resulted in a typical energy resolution at the peak of the ${}^7\text{Li}$ curve of 2 MeV, and a worst case resolution for the lowest

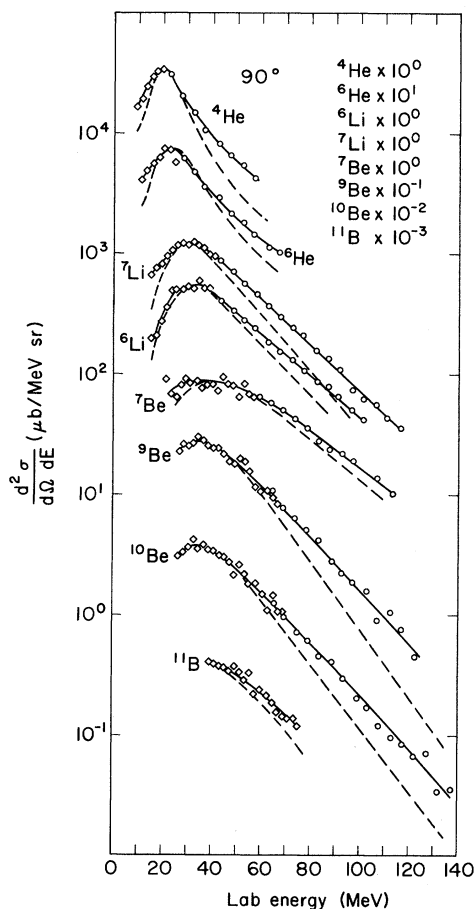


FIG. 2. Laboratory energy spectra at 90° for α and proton irradiations. The incident proton data are shown as dashed curves and have been normalized to their peaks to the incident α data.

energy ${}^{11}\text{B}$ fragments of 6 MeV. The data show gross features already noted for proton irradiations⁶:

(1) The peaks in the spectra shift towards higher energy as the atomic numbers of the fragments increase, in accord with an increasing Coulomb barrier.

(2) The spectra of the neutron-deficient isotopes ${}^6\text{Li}$ and ${}^7\text{Be}$ exhibit more prominent high-energy tails that do the other isotopes of these elements.

Laboratory angular distributions are shown in Fig. 3. Shown with the proton-induced data are the previously published data⁶ at five angles, showing that a straight line through the data is adequate for integration. The distributions were integrated according to the straight lines drawn between the data points to give the total cross sections and the forward-backward ratios F/B listed in Table II. Since double differential cross sections for the deuteron bombardments were measured only at 90° , an estimate for the ratios of deuteron-to-proton-induced total cross sections was made on the basis of the ratio curves in Fig. 1. Cross sections for some rarer isotopes were obtained by comparing systematics of ratios of peak areas in the 90° particle spectra of both the deuteron and α data to that of the proton data. The ratios obtained are listed in Table II, along with approximate total cross sections for each fragment from the α particle exposure obtained by using the published proton-induced cross sections.

Examining Table II one again notes that the total

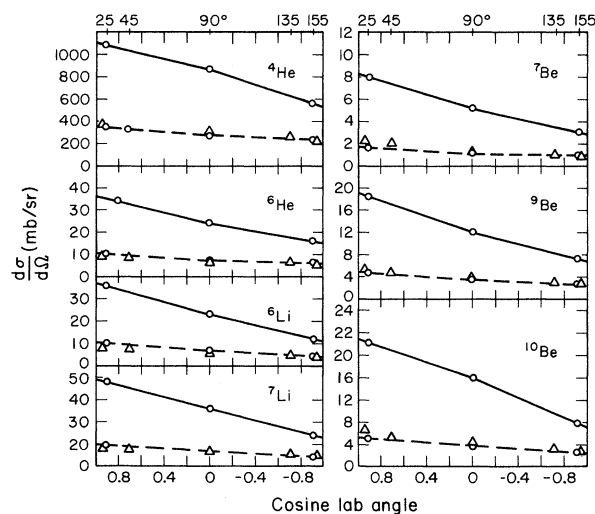


FIG. 3. Laboratory angular distributions for α - and proton-induced reactions. The dashed lines go through the incident proton data. The circles are from the present work while the data represented by triangles come from Ref. 6.

TABLE II. Total cross sections for the α -induced reactions and ratios of α - and deuteron-induced reactions to proton-induced reactions. F is the fraction of events going into the forward hemisphere in the laboratory system and B is the fraction in the backward hemisphere.

Isotope	σ_α (mb)	σ_α/σ_p	σ_d/σ_p	$(F/B)_\alpha$	$(F/B)_\alpha/(F/B)_p$
^4He	10 600	2.9	1.4 ^a	1.41	1.13
^6He	310	3.1	1.5 ^b	1.48	1.13
^6Li	297	3.3	1.3 ^b	1.75	1.14
^7Li	650	3.8	1.5 ^a	1.67	1.12
^8Li	≈ 210	4.2 ^b	1.2 ^b		
^9Li	≈ 60	3.8 ^b	1.5 ^b		
^7Be	67	4.3	1.5 ^a	1.7	1.1
^9Be	157	3.4	1.3 ^a	1.64	1.22
^{10}Be	196	4.0	1.6 ^a	1.67	1.14
^{11}Be	≈ 21	4.3 ^b			
^{12}Be	≈ 11	4.5 ^b			

^a Based solely on the 90° differential cross sections.

^b Based solely on the ratios of peak areas in the 90° particle spectra.

cross sections for both the α particle and the deuteron reactions are larger than the corresponding proton reactions. In addition, a somewhat greater increase in cross section is noted for the heavier fragments than for the lighter ones. The F/B ratios for the α particle irradiation show forward peaking of the laboratory angular distributions. The ratio of the F/B ratios for the α -induced and proton-induced reactions given in Table II shows the α particle reactions to be uniformly slightly more forward peaked, with the average ratio of F/B ratios equal to 1.14.

Significant contributions to the experimental errors on the results presented were made by the following:

(1) *Statistics*: The statistical errors in the double differential cross sections at 90° can be seen by the fluctuations of the data points in Fig. 2. The data at the forward and backward angles were of poorer quality but probably do not contribute significantly to the errors in the total cross sections, because these are determined mainly by the 90° data.

(2) *Extrapolations and interpolations*: Usually little extrapolation was necessary in obtaining the differential cross sections presented in Fig. 3. In the worst cases, at the backward angle, the extrapolated area was no more than 25% of the total and probably contributed less than 10% to the final error. It is estimated that the straight line interpolation procedure used to integrate the angular distributions introduces about a 10% uncertainty in the total cross section for the α particle reac-

tions.

(3) *Beam monitoring*: The beam monitoring exhibited a reproducibility of 5%.

(4) *Absolute normalization*: All of the cross sections are systematically dependent on the value for the differential ^4He cross sections from 5.5 GeV protons on U. As indicated in Ref. 6, this value is based on a radiochemical determination of ^7Be accurate to 9%.

In summary the experimental errors on the total cross sections presented in Table II are approximately 15%, to which must be added the 9% error in the monitor cross section. The numbers preceded by an approximate sign, which were obtained from the 90° particle identifier spectra, are probably only accurate to 25%. In the deuteron irradiations the beam monitoring was not as accurate and all of those ratios may be uncertain by 25%.

IV. DISCUSSION

As in Ref. 6 an attempt was made to fit the energy spectra in terms of an evaporation model in order to extract certain parameters, such as effec-

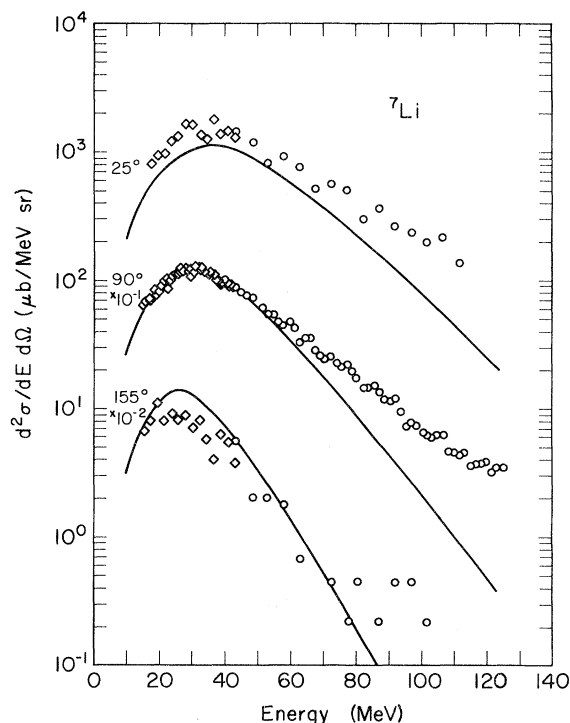


FIG. 4. The ^7Li data from incident α particles together with curves calculated with the following parameters: $B = 32$ MeV, $\langle k \rangle = 0.48$, $\Delta = 0.38$, $\tau = 12.0$ MeV, $\langle v \rangle = 0.005$, and $n = 2$. The curves have been normalized to the data only at the peak of the 90° spectrum. The points and curves have been lowered by one decade at 90° and two decades at 155°.

TABLE III. Parameters obtained in the curve fitting.

Isotope	B (MeV)	$\langle k \rangle \pm \Delta$	Incident protons 90°			$\langle v \rangle / c^b$	$\langle k \rangle \pm \Delta$	Incident α particles 90°			$\langle v \rangle / c$ (MeV)
			peak energy (MeV)	τ (MeV)	τ_T^a (MeV)			peak energy (MeV)	τ (MeV)	τ_T^a (MeV)	
^4He	22	0.58 ± 0.2	20	6	19	0.003	0.48 ± 0.3	20	6.5	16	<0.01
^6He	22	0.60 ± 0.1	24	9	16		0.50 ± 0.3	23	10	18	<0.01
^6Li	32	0.57 ± 0.1	32	13	18	0.006	0.52 ± 0.2	33	13.5	19	<0.02
^7Li	32	0.58 ± 0.25	31	10	15	0.005	0.48 ± 0.38	30	12	19	<0.01
^7Be	42	0.54 ± 0.25	41	17	19	0.007	0.48 ± 0.35	37	19	22	<0.03
^9Be	41	0.58 ± 0.05	36	12	13	0.007	0.48 ± 0.15	35	13.5	19	<0.01
^{10}Be	41	0.58 ± 0.05	36	12	15	0.007	0.52 ± 0.15	35	13.5	17	<0.01
^{11}Be	50			13		0.006			15		

^a τ_T refers to the temperature needed to fit the high-energy tail of the spectrum.

^b Data from Ref. 6.

tive Coulomb barriers (kB) and apparent nuclear temperatures (τ). The Maxwellian form used was:

$$P(\epsilon) = (\epsilon - kB)e^{-(\epsilon - kB)/\tau}, \quad \epsilon > kB,$$

where the values of k were smeared uniformly around the average value $\langle k \rangle$ by an amount $\pm \Delta$. The nominal Coulomb barrier B was calculated for tangent spheres with a radius parameter of 1.4 fm and with the assumption that the emitting nucleus was ^{220}Rn . The energies were corrected for recoil with this same assumption. In the present experiment the target was fairly thick. The energy spectra were corrected for the degradation in half the target thickness. The smearing due to the target thickness was introduced into the calculated curves before they were compared to the experiment. In this way the parameters extracted from the fitting procedure are the ones one would have obtained if the target had been negligibly thin. An example of the fit is shown in Fig. 4, and the parameters obtained are listed in Table III. For the 90° data the apparent temperature τ is obtained from the slope just above the peak, the fraction of the effective Coulomb barrier $\langle k \rangle$ from the peak position, and the smearing Δ is not the uncertainty in $\langle k \rangle$ but only the smearing of k needed to fit the lowest energy points. Still, the curve only fits near the peak, and the limiting temperature needed to fit the highest energies measured is also listed in Table III as τ_T . The parameters obtained with incident protons are consistent with those obtained previously. Because of the poor quality of the data at 25° and 155°, the average forward velocity of the emitting system $\langle v \rangle$ and the correlation parameter n which describes the spread in this quantity, were taken from the previous study with incident protons.⁶ The value of n was taken equal to 2 and the $\langle v \rangle$ values are shown in the table. The peak

energies of the calculated curves at the forward and backward angles are not inconsistent with the data, which means that the $\langle v \rangle$ values are not very different than with incident protons, although we have only listed upper limits in Table III. The discrepancy in Fig. 4 in the heights of the forward and backward curves indicates that the fragments are forward peaked in the system of the emitting nucleus. This effect is more pronounced than observed previously with incident protons.⁶ From Table III it can be seen that the effective Coulomb barriers which were already anomalously low with incident protons, have dropped another 15% for incident α particles. The apparent temperatures, which were unbelievably high for incident protons, have climbed another $1\frac{1}{2}$ MeV on the average for incident α particles. And finally, the smearing parameters have increased almost a factor of 2.

Note added in proof: One can calculate the total reaction cross sections¹¹ knowing the radii of the deuteron and α particle.¹² The results for protons, deuterons, and α particles on U are 1.91, 2.29, and 2.48 b, respectively. Thus the fragment yields are considerably enhanced even relative to the total reaction cross sections. In fact, the 10.6 b cross section for ^4He indicates that there are on the average 4.3 evaporation α particles per α interaction in U.

V. CONCLUSIONS

We have compared the interaction of multi GeV protons, deuterons, and α particles with a uranium nucleus. Although the cross sections for the production of fragments from uranium are a factor of 1.5 higher with deuterons than with protons, the energy spectra of these fragments are not significantly different. However, in the interaction of α particles with uranium there are many indi-

cations of increased deposition energy. The cross sections for producing the fragments are a factor of 3 to 4 higher. The effective Coulomb barriers are lower, the apparent temperatures are higher, the smearing of the energy spectra has increased, and the angular distributions are more forward peaked. It would of course be desirable to continue these studies with heavier incident ions, especially in light of the indications in the data of Sullivan *et al.*³

ACKNOWLEDGMENTS

We wish to thank Earl K. Hyde for assisting in parts of this experiment. We especially appreciate the very important ion chamber calibrations, cheerfully and efficiently performed by Al Smith, with the assistance of Joe McCaslin. We wish also to thank Richard Morgado who designed the multi-wire proportional chamber.

*Work done under the auspices of the U. S. Atomic Energy Commission.

†Present address: Los Alamos Scientific Laboratory, Los Alamos, New Mexico 87544.

‡Permanent address: University of Maryland, College Park, Maryland 20742.

¹H. Steiner, in *Particle Physics, Proceedings of the Adriatic Meeting, Rovinj, 1973*, edited by M. Martinis, S. Pallua, and N. Zovko (North-Holland, Amsterdam, 1974), p. 69; E. K. Hyde, Lawrence Berkeley Laboratory Report No. LBL-3049, 1974 (unpublished); *Physica Scripta* (to be published); H. H. Heckman, in *High-Energy Physics and Nuclear Structure, Proceedings of the Fifth International Conference on High-Energy Physics and Nuclear Structure, Uppsala, Sweden, 1973*, edited by G. Tibell (North-Holland, Amsterdam, 1974), p. 403.

²P. J. Lindstrom, D. E. Greiner, H. H. Heckman, B. Cork, and F. S. Bieser, Lawrence Berkeley Laboratory Report No. LBL-3650, 1975 (unpublished); J. Jaros, J. Papp, L. Schroeder, J. Staples, H. Steiner, and A. Wagner, Lawrence Berkeley Laboratory Report

No. LBL-2115, 1973 (unpublished).

³J. D. Sullivan, P. B. Price, H. J. Crawford, and M. Whitehead, *Phys. Rev. Lett.* **30**, 136 (1973).

⁴S. K. Chang and N. Sugarman, *Phys. Rev. C* **9**, 1138 (1974); Y. W. Yu and N. T. Porile, *ibid.* **10**, 167 (1974).

⁵V. P. Crespo, J. M. Alexander, and E. K. Hyde, *Phys. Rev.* **131**, 1765 (1963); R. G. Korteling and E. K. Hyde, *ibid.* **136**, B425 (1964); P. J. Karol, *Phys. Rev. C* **10**, 150 (1974).

⁶A. M. Poskanzer, G. W. Butler, and E. K. Hyde, *Phys. Rev. C* **3**, 882 (1971).

⁷E. K. Hyde, G. W. Butler, and A. M. Poskanzer, *Phys. Rev. C* **4**, 1759 (1971); R. G. Korteling, C. R. Toren, and E. K. Hyde, *ibid.* **7**, 1611 (1973).

⁸W. Scheid, H. Muller, and W. Greiner, *Phys. Rev. Lett.* **32**, 741 (1974); C. Y. Wong and T. A. Welton, *Phys. Lett.* **49B**, 243 (1974).

⁹H. Bichsel and C. Tschaler, *Nucl. Data* **A3**, 343 (1967).

¹⁰A. Smith and J. McCaslin, unpublished data.

¹¹R. W. Williams, *Rev. Mod. Phys.* **36**, 815 (1964).

¹²L. C. Vaz and J. M. Alexander, *Phys. Rev. C* **10**, 464 (1974).